

Biomechanical analysis of Oligochaeta crawling

Dino Accoto, Piero Castrataro*, Paolo Dario

CRIM Lab., Polo Sant'Anna Valdera, Scuola Superiore Sant'Anna, Viale R. Piaggio, 34, 56025 Pontedera (PI), Italy

Received 16 March 2004; received in revised form 26 March 2004; accepted 28 March 2004

Available online 8 June 2004

Abstract

Hydrostatic skeletons, such as that of Oligochaeta and Hirudinea, allow the locomotion of animals with soft segmented bodies. In this paper crawling of Oligochaeta, and in particular that of earthworm (*Lumbricus terrestris*), is analyzed from a biomechanical point of view, starting from the experimental kinematic description of deformations coupled with a simple friction model. The analysis is able to predict crawling velocity with an error of about 15% with respect to the experimental measured values. Also muscular stress during locomotion is evaluated and found to be compatible with biological values.

© 2004 Elsevier Ltd. All rights reserved.

Keywords: Hydrostatic skeleton; Oligochaeta; Biomechanics

1. Introduction

Body segmentation is the hallmark of the three classes encompassed in the Annelida phylum: Polychaeta, Oligochaeta and Hirudinea. Each body segment (metamere) acts as a module of the hydrostatic skeleton, which comprises a deformable body wall (cuticle), soft tissues and incompressible *coelomic* fluid. The coelomic fluid enables antagonism of muscles and stiffening of the organism. Peristaltic locomotion is the characteristic deambulatory mode of Oligochaeta and it arises from the alternating contraction and relaxation of longitudinal and circumferential muscles. The contraction of longitudinal muscles expands segments radially, while the contraction of radial muscles causes the axial elongation of the segments. This means that motion in hydrostats is primarily based on changes in the dimension of body segments. A detailed phenomenological description of this mechanism is given by Gray (1968). A rather common example of Oligochaeta is the earthworm (*Lumbricus terrestris*), to whom we will extensively refer in the following.

Biomechanical models of the crawling by hydrostatic skeletons have been proposed by several Authors. Keller

and Falkovitz (1983) presented a model that takes into account friction, gravity, and tension. The equation of motion is formulated using the concept of periodic travelling waves and resolved taking into consideration that tension, linear density and time rate of change of tension are required to lie between prescribed bounds, but no direct reference to detailed experimental kinematic observation is made.

Dobrolyubov (1986) presented a purely kinematic model, based on a longitudinal strain function, describing the interaction between the substrate and deformable elongated bodies, along which waves of longitudinal deformation travel.

Wadepuhl (1989) presented a numerical model based on the assumption that the constitutive equation of muscular layers (deformation/force relation) is linear elastic. The skeleton model is assumed to deform so that the potential energy stored in the elastic elements is minimized. This shape is calculated as equilibrium state by using finite element methods and optimization techniques.

Chirikjian and Burdick (1995) considered the kinematics of hyper-redundant robot locomotion over uneven solid terrain, and presented algorithms to implement a variety of gaits similar to those of inchworms, earthworms, snakes and slugs. Many of these forms of undulatory biological locomotion can be idealized as travelling or stationary waves of body

*Corresponding author. Tel.: +39-050-883403; fax: +39-050-883402.

E-mail address: piero@sssup.it (P. Castrataro).

deformation. The developed analysis and algorithms are based on a continuous backbone curve model which captures the animal movement. The locomotion algorithms can be used to plan the manipulation of objects which are grasped in a tentacle-like manner.

Skierczynski et al. (1996) presented a model of the hydrostatic skeleton of the leech (Hirudinea class) aimed to predict the shape and the pressure within the animal in response to a given pattern of motor neurons activity in different behaviors. The model was implemented to simulate the vermiform elongation of the leech, predicting the shape and the pressure changes during locomotion. The theoretical predictions are in good agreement with experimental results.

The goal of this paper is to propose a biomechanical analysis of Oligochaeta crawling based on purely experimental kinematic observations. The obtained results, in terms of velocity and muscular stress, are compared to experimental values. The biomechanical analysis is based on a continuity equation coupled to a simple friction model. Internal pressure is not considered, because no experimental data are available. The energetics of locomotion, already investigated (see Casey, 1991; Walton et al., 1990), is not considered.

2. Analysis of deformations

Fig. 1 depicts the two main muscular systems of the earthworms (*Lumbricus terrestris*). The cuticle covers a layer of circumferential muscles, whose contraction causes a radial shrinking and a longitudinal elongation of the segments. Longitudinal muscles, located beneath circumferential muscles, act antagonistically, causing a longitudinal contraction and a radial expansion. An earthworm has about 150 segments, which are deformed by the alternating action of longitudinal and circumferential muscles. The contraction of segmental muscles is not synchronous. Each segment is deformed with some delay with respect to its neighbors, so that the collective behavior of all the segments produces a peristaltic wave moving from the tail to the head. More precisely, two peristaltic waves may be identified: a longitudinal wave, corresponding to the contraction of longitudinal mus-

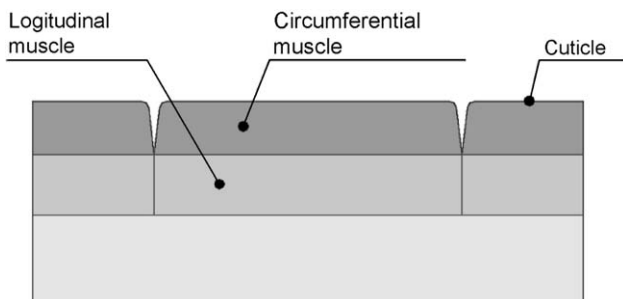


Fig. 1. Longitudinal and circumferential muscle in a segment.

cles, and a radial wave, corresponding to the contraction of radial muscles.

The starting point of our analysis is the determination of a relation between radial and longitudinal deformations. In particular, we assume that each segment can be approximated by a round cylinder with constant volume, so that a radial contraction is accompanied by an elongation, in order to keep the volume unchanged.

According to these hypotheses, the relation we are looking for is but a *continuity equation*, in the sense that, given a radial deformation, we calculate the longitudinal deformation that keeps the volume of each segment unchanged. Notably, no reference to the smallness of the deformation is done.

Referring to Fig. 2, we define our displacement functions over the domain $[0, L]$, which corresponds to the configuration of the earthworm (in the following indicated concisely with the symbol E) at a reference instant, namely $t = 0$. The axial coordinate will be x . We will denote by $\Delta(x, t)$ the axial displacement of a point that was in x at $t = 0$. The radius of a generic cross section will be denoted by $r(x, t)$. Obviously, although the length of E changes in time, because of the axial displacement $\Delta(x, t)$, the reference domain $[0, L]$, which refers to the reference configuration at $t = 0$, is fixed.

In the reference configuration, we consider two points on the axis of E , respectively A_0 in \bar{x} and B_0 in $\bar{x} + dx$. In the generic instant t , the points have moved to A_1 and B_1 . At the instant $t + dt$, the points will be in A_2 and B_2 . Taking into consideration the axial displacement function, $\Delta(x, t)$, the locations of the six points are given as follows:

$$\begin{aligned} A_0 &= \bar{x}, \\ B_0 &= \bar{x} + dx, \\ A_1 &= \bar{x} + \Delta(\bar{x}, t), \\ B_1 &= \bar{x} + dx + \Delta(\bar{x} + dx, t), \\ A_2 &= \bar{x} + \Delta(\bar{x}, t + dt), \\ B_2 &= \bar{x} + dx + \Delta(\bar{x} + dx, t + dt). \end{aligned} \quad (1)$$

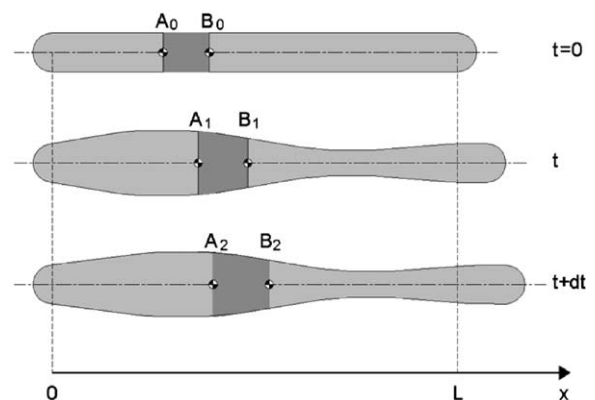


Fig. 2. The Reference configuration at $t = 0$ (top) and two generic configurations at t and $t + dt$.

Since the volume of the segment between A_j and B_j ($j = 0, 1, 2$) must be constant, we obtain, after eliminating higher-order infinitesimals:

$$\frac{\partial}{\partial t}(r^2) + \frac{\partial}{\partial t}\left(r^2 \frac{\partial \Delta}{\partial x}\right) = 0. \quad (2)$$

We can now integrate Eq. (2) in time

$$r^2\left(1 + \frac{\partial \Delta}{\partial x}\right) = f(x), \quad (3)$$

where $f(x)$ is an arbitrary function.

By definition, $\Delta(x, 0) = 0$ (displacements are measured with respect to the reference configuration). So we can write

$$f(x) = r^2(x, t = 0) = r_0^2(x). \quad (4)$$

Substituting Eq. (4) into Eq. (3) we finally find

$$r^2(x, t)\left(1 + \frac{\partial \Delta}{\partial x}(x, t)\right) = r_0^2(x), \quad (5)$$

$\Delta(x, t)$ can be derived from $r(x, t)$ using Eq. (5)

$$\Delta(x, t) = \Delta(0, t) + \int_0^x \left(\frac{r_0^2(k)}{r^2(k, t)} - 1\right) dk. \quad (6)$$

The choice of the function $\Delta(0, t)$ is not arbitrary, because the center of mass of E must have a constant velocity when no external force is considered. In particular we will suppose that the center of mass was at rest at $t = 0$. So it must be ($\forall t$):

$$\int_0^L \pi \rho x r_0^2(x) dx = \int_0^L \pi \rho [x + \Delta(x, t)] r_0^2(x) dx \quad (7)$$

which simplifies in

$$\int_0^L \Delta(x, t) r_0^2(x) dx = 0. \quad (8)$$

By introducing the quantity

$$\Psi = \int_0^L r_0^2(x) dx \quad (9)$$

and by substituting Eq. (6) in Eq. (7), we obtain

$$\Delta(0, t) = -\frac{1}{\Psi} \int_0^L \left[\int_0^x \left(\frac{r_0^2(k)}{r^2(k, t)} - 1\right) dk \right] r_0^2(x) dx. \quad (10)$$

3. Friction model

The relation between axial and radial displacements given by Eqs. (5) and (10) respects the conservation of mass and momentum. Anyhow, the description of the deformation of E is not enough to describe the crawling until the external forces (friction) are introduced in the analysis. The obvious reason is that deformations provide internal forces, which do not modify the momentum of the center of mass of E . In this paragraph we complete the dynamic model by introducing the

frictional properties of the rigid substrate on which E is supposed to crawl.

The tribology of contact between a soft-bodied organism and a substrate is by no means trivial, and an accurate description of frictional force is beyond the aim of this paper. Possibly the simplest frictional model has been assumed here to focus on the biomechanics of locomotion instead of on the tribology of contact. Coulombian friction for incipient motion is assumed between E and the substrate. Following this model, a segment experiences a frictional force which is directly proportional to its weight. The proportionality factor is assumed to be constant and it is indicated by μ (friction coefficient).

A generic segment in the reference configuration, comprised between the sections x and $x + dx$, has a constant mass: $dm = \pi \rho g r_0^2(x) dx$. Although the shape of E changes in time, a generic segment provides a frictional force that has constant modulus, while its sign depends on the velocity, v , of the segment: $dF_a = \mu \rho g \operatorname{sgn}(v) dm$, where $\operatorname{sgn}(x)$ denotes the sign function valued -1 if $x < 0$, 1 if $x > 0$, 0 otherwise. In a generic instant t the total frictional force is

$$F_a = - \int_0^L \mu \rho g \pi r_0^2(x) \operatorname{sgn}(v) dx. \quad (11)$$

We indicate with A the point of E that is at $x = 0$ in the reference configuration. The velocity of a generic point P is: $v_P = v_A + v_{PA}$, where v_A is the velocity of A and v_{PA} is the velocity of P relative to A . Evidently

$$v_P = v_A + \dot{\Delta}(x, t) - \dot{\Delta}(0, t). \quad (12)$$

The total frictional force (11) can be written as

$$F_a = - \int_0^L \mu \rho g \pi r_0^2(x) \operatorname{sgn}[v_A(t) + \dot{\Delta}(x, t) - \dot{\Delta}(0, t)] dx. \quad (13)$$

In Eq. (13) v_A is the only unknown function, and it can be evaluated by considering the dynamic equilibrium of E :

$$F_{inertia} = F_a.$$

The inertial force is

$$F_{inertia} = \int_0^L \pi \rho r_0^2(x) [v_A + \ddot{\Delta}(x, t) - \ddot{\Delta}(0, t)] dx. \quad (14)$$

If we expand the dynamic equation ($F_{inertia} = F_a$) using Eq. (8) and using the quantity Ψ defined in Eq. (9) we finally get

$$\begin{aligned} \dot{v}_A - \ddot{\Delta}(0, t) &= -\frac{\mu g}{\Psi} \int_0^L r_0^2(x) \operatorname{sgn}[v_A + \dot{\Delta}(x, t) - \dot{\Delta}(0, t)] dx. \end{aligned} \quad (15)$$

4. Experimental input

Quillin (1999) reported an exhaustive set of experimental data referring to the kinematic scaling of a generic locomotion-related feature (p) of *Lumbricus terrestris*. A generic feature p is interpolated in the form: $p = am^b$, where m is the mass, while a and b are experimentally evaluated parameters. The units used are mm , s and $grams$. Quillin’s extensive sets of interpolated data are well suited to be used in a biomechanical model of crawling locomotion. Indeed, they allow quite easily to find an analytical expression of $r = r(x, t)$ that takes into account the measurements performed on the biological models. In particular, the radius of a segment at $x = \bar{x}$ is depicted in Fig. 3. The function $\bar{r}(t) = r(\bar{x}, t)$ is initially constant (R_0). At time T ($T = 4.0m^{-0.07}$) it becomes periodic with period T . The following variables are defined:

- t_{lc} : time for longitudinal contraction; $t_{lc} = -\varepsilon_z/\varepsilon_{z\dot{c}}$ where ε_z is the longitudinal strain ($|\varepsilon_z| = 0.60$, independent from mass) and $\varepsilon_{z\dot{c}}$ is longitudinal strain rate during contraction ($\varepsilon_{z\dot{c}} = 0.75m^{-0.06}$);
- t_{str} : stance time at maximum radius; $t_{str} = 1.6m^{0.04}$;
- t_{cc} : time for circumferential contraction; $t_{cc} = -\varepsilon_\theta/\varepsilon_{\theta\dot{c}}$ where ε_θ is the circumferential strain ($|\varepsilon_\theta| = 0.25$, independent from mass) and $\varepsilon_{\theta\dot{c}}$ is circumferential strain rate during contraction ($\varepsilon_{\theta\dot{c}} = 0.41m^{-0.09}$);
- t_{str} : stance time at minimum radius; $t_{str} = T - t_{lc} - t_{str} - t_{cc}$;
- v : variation of radius; $v = |\varepsilon_\theta|/(2 + |\varepsilon_\theta|) = 0.1429$.

By referring to Fig. 3, the horizontal segments, at R_0 , $R_0(1 + v)$ and $R_0(1 - v)$ have been simply connected via sinusoidal tracts, so that $r(x, t) \in \mathcal{C}^1$, i.e. it is a continuous function with continuous first derivatives. Fig. 3 shows how r changes in time for a given $x = \bar{x}$. The radius wave function translates in space with a velocity that can be evaluated from Quillin’s data. If we denote the frequency of the wave by f ($f = 0.25m^{0.07}$), translational velocity is $v = Lf$ and we can write: $r(x, t) = \bar{r}(t + x/v)$.

5. Numerical results

The dynamic model (15) with the initial condition: $v_A(0) = 0$ has been implemented in a dedicated software

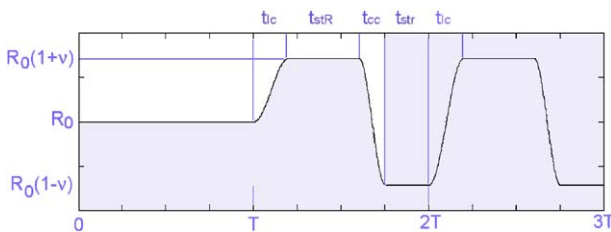


Fig. 3. Radius of a segment as a function of time. The meaning of the symbols used for the definition of $r(x, t)$ are shown.

for numerical calculation using the radial wave function $r(x, t)$ described above. Space and time have been discretised with a constant mesh having 300 elements in space (about twice the number of segments in *Lumbricus terrestris*) and with a time step of $6 \times 10^{-4}s$. These values have been chosen experimentally, since they allow repeatable results with negligible numerical sensitivity. Simulations have shown that $v_A(t)$ reaches its final regime after a time of about 2 T. For this reason, 3 full periods have been simulated, and v_A has been averaged over the last period to get the mean translation velocity of E . No advantage in terms of accuracy arises if the temporal horizon is extended. The integration has been performed using direct first-order Euler method.

The values of m taken into account are: 0.01, 0.1, 0.3, 0.5, 1, 2, ..., 9. For each m , a simulation has been performed using 4 different values of μ ranging from extremely low to quite large values (0.01, 0.1, 0.3, 0.5). Also the trivial case $\mu = 0$ has been taken into consideration, leading to negligible average velocities $v_A \approx 10^{-3}$ mm/s, due to numerical errors. Quite interestingly, very small values of $\mu \neq 0$ are enough to allow the locomotion of E , and the calculated velocity is constant with μ (variations less than 2%) over the large span of friction coefficients taken into account.

Fig. 4 shows the results of the simulations plotted against the expected velocities. The obtained data can be fit using an exponential function: $v_A = \alpha m^\beta$ with $\alpha = 4.07$ and $\beta = 0.20$ ($R^2 = 0.994$). Comparing with Quillin’s interpolation: $v = 3.8m^{0.33}$ it is evident that the maximum error occurs for very small masses (94% for $m = 10^{-2}g$) and that it decreases quickly with increasing

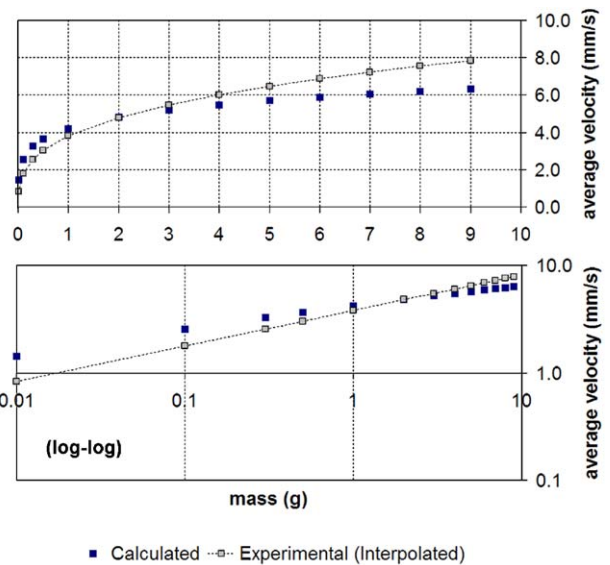


Fig. 4. Comparison between numerical results and interpolated experimental data. Top: linear scales; bottom: log–log scales.

masses. In the range $m \in [10^{-2}g, 9g]$ the root mean square error is 15.3%, which is an acceptable value given the variability of experimental data.

Finally, internal stresses acting on the longitudinal and circumferential muscles have been calculated and compared to those experimentally measured. In particular, in Quillin (1998) two geometric parameters can be defined (Fig. 1):

- t_s mid-segment thickness, i.e. sum of the circumferential muscle thickness and the longitudinal muscle thickness ($t_s = 0.31m^{0.42}$)
- t_a annulus thickness, i.e. longitudinal muscle thickness ($t_a = 0.19m^{0.45}$).

From these parameters we can derive:

- A_c circumferential muscle area: $A_c = L(t_s - t_a)$, where L is the length of a segment),
- A_l longitudinal muscle area: $A_l = 2\pi t_a(r_0 - t_s + t_a/2)$.

Longitudinal stress, σ_x , can be easily evaluated by considering the equilibrium to the translation of the part of E between $x = 0$ and $x = \bar{x}$. In this evaluation the resultant of circumferential stresses acting on the section at $x = \bar{x}$ balances the resultant of external forces, i.e. friction and inertia. Circumferential stresses, σ_θ , can be calculated from σ_r by using: $\sigma_\theta = 2\sigma_x$. This expression can be easily obtained by considering the equilibrium of a single segment, in which the pressure of the *coelomic* liquid is acting. The stress σ_x has been calculated numerically in the worst condition ($\mu = 0.5$) for the whole range of masses already considered. The maximum stress occurs at the central segment, whose elongation causes the translation of half the body of E . On the contrary, σ_x approaches zero at the extremities of E because the associated mass tends to disappear. In particular, if we plot the maximum σ_x for each segment during a full cycle, we have a triangular diagram with $\sigma_x = 0$ at the extremities and a maximum value at the middle. The diagram of minimum stresses has, as expected, the same behavior, but the minimum value, reached again at the central segment, has the same intensity as the maximum stress but opposite sign. If we plot maximum and minimum stresses (reached at the central segment) for the whole set of masses m simulated, we obtain the diagram shown in Fig. 5.

6. Discussion

Hydrostatic skeletons, as those of *Lumbricus terrestris* and other Annelida, show a rather simple biomechanical structure, based on the serial linking of basic modules, the segments, with identical anatomy and physiology. Circumferential and longitudinal muscles contract

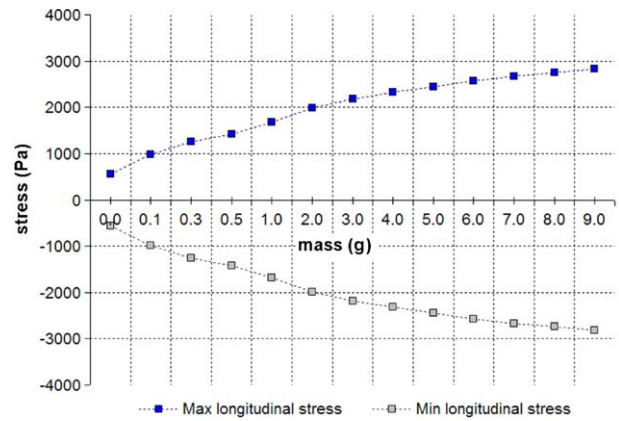


Fig. 5. Maximum and minimum longitudinal stresses during locomotion for differently sized earthworms.

antagonistically with rigorous cadence, thus producing a peristaltic wave. When a peristaltically moving hydrostatic body is in contact with a rigid substrate, which is able to exert frictional forces, locomotion occurs, and a periodic velocity regime is quickly reached after about two full periods of the peristaltic wave. This paper attempted to focus purely on the biomechanics of the locomotion, starting from a biomimetic description of the longitudinal and radial waves. The basic hypothesis, i.e. the constance of volume of each segment, derives from the incompressibility of the *coelomic* liquid encompassed in each segment, and it is a commonly accepted starting point in the description of peristaltic locomotion by hydrostatic animals.

The second hypothesis formulated concerns the type of friction occurring at the interface between the Earthworm and the ground. It has been assumed that Coulombian friction model applies, in the condition of incipient motion. In other words, it is assumed that each segment is subject to a frictional force proportional to its weight, and that the proportionality coefficient, indicated by μ , is constant. Since a segment changes its shape but not its weight, the frictional force acting on a segment has a constant intensity during motion, while its direction changes in order to be always opposite to the relative velocity to ground. The friction model is probably the simplest conceivable and it may be criticized for this reason. Indeed, the actual value of friction forces in Coulomb's model is unknown until motion becomes incipient. Only in this situation (beginning of sliding with respect to the ground) the value of friction becomes known. The use of a simplified friction model is nevertheless acceptable given the large number of segments taken into account. The reason is that during crawling the majority of segments are in the sliding situation, and those not sliding yet are subject to a frictional force of the same order of magnitude of that modelled. As expected, the choice of the simple

expression of friction, causes unreliable velocities during the initial instants of motion. After a quite short lapse of time (less than two full periods of the peristaltic wave) the velocity profile reaches the asymptotic regime, already presented, with an average locomotion velocity which differs from the experimental one by about 15%.

The good agreement of numerical and experimental data allows us to conclude that the simple friction model used ultimately catches the physics behind peristaltic locomotion. In particular, Fig. 6 plots velocity, expressed as *body* lengths s^{-1} , vs. mass (g). As found in Quillin (1999) all data are in the range 0.04 ± 0.02 , except for very small masses (< 0.01 g) where the analytical description given in this paper fails significantly.

Friction model, as it has been presented here, implicitly assumes that the whole weight of each segment is balanced by a normal reaction provided by the rigid substrate. Since a generic segment is connected to two adjacent segments (obviously this is not true for the two extremal segments), we are silently assuming that the hydrostatic skeleton has negligible bending rigidity. This assumption is not particularly strong because the hydrostatic slender skeleton does not have a significant bending stiffness.

One of the most interesting result obtained by numerically solving the equation of the dynamic model is that no specific tribological properties of the contact between the body and the substrate must be assumed in order to match experimental data. Indeed, the contact with the rigid substrate has been modelled using one single parameter: the friction coefficient μ . In addition, the choice of μ does not significantly affect the final mean velocity of the crawler. This result is not trivial, since it is known that Earthworms have setae on ventral parapodia to improve locomotion ability (Ruppert and Barnes, 1994). We may conclude that the role of such setae is not of fundamental importance to locomotion, which would seemingly occur on a smooth surface, provided that the contact between the surface and the body has a non-zero friction coefficient. In fact, low-friction coefficients assures the same asymptotic kinematic behavior with reduced energy dissipation.

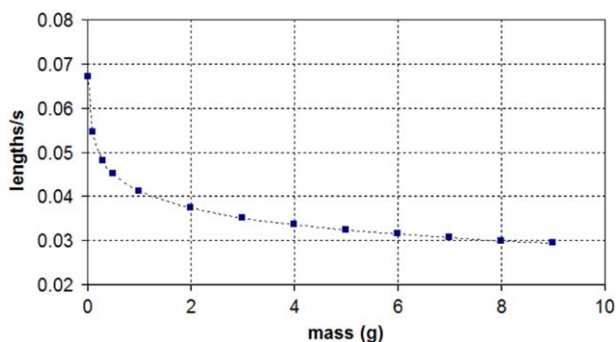


Fig. 6. Crawling velocity expressed as s^{-1} .

If there is no biomechanical limitation to the lower value of μ , the upper value is given by the maximum value of longitudinal and circumferential stress acting on the muscles. The developed model allows a quick evaluation of the stresses acting on the muscles by simply considering the equilibrium of a generic tract of the body under the effect of internal and external forces. The stresses have been evaluated in correspondence of a quite high value of μ (0.5). Nevertheless, the obtained values are acceptable from a biomechanical point of view, as they do not exceed 3 kPa (Fig. 5) and 6 kPa, respectively, for longitudinal and radial stresses. This result may be seen as a further positive validation of the model, because it shows that not only kinematic quantities (i.e. strain and velocities) are compatible with experimental one, but also dynamic quantities.

7. Conclusion

In this paper a biomechanical model for the locomotion of crawlers with hydrostatic skeletons has been presented. Kinematics parameters for the description of the peristaltic wave have been taken from already known experimental observations. The obtained velocity is in good agreement with observed data, with an error of about 15%. Higher discrepancies in velocity values occur for small animals (mass below 0.1 g). A simple model for friction has been used and discussed, based on the assumption that a single friction coefficient is sufficient to describe frictional forces. The value of the chosen friction coefficient does not affect the final regime average velocity. Finally, internal muscle stresses have been evaluated and found to be completely compatible with biological limits.

Acknowledgements

The activity presented in this paper has been carried on with the support of the European Commission, in the framework of the BIOLOCH Project (BIOMimetic structures for LOComotion in the Human body IST FET Programme, IST-2001-34181).

References

- Casey, T.M., 1991. Energetics of caterpillar locomotion: biomechanical constraints of a hydraulic skeleton. *Science* 252, 112–114.
- Chirikjian, G.S., Burdick, J.W., 1995. The kinematics of the hyper-redundant robot locomotion. *IEEE Trans. Robot. Automat.* 11 (6), 781–793.
- Dobrolyubov, A.I., 1986. The mechanism of locomotion of some terrestrial animals by travelling waves of deformation. *J. Theor. Biol.* 119, 457–466.
- Gray, G., 1968. *Animal Locomotion*. W. W. Norton, New York.
- Keller, J.B., Falkovitz, M., 1983. Crawling of worms. *J. Theor. Biol.* 104, 417–442.

- Quillin, K.J., 1998. Ontogenetic scaling of hydrostatic skeletons: geometric, static stress and dynamic stress scaling of the earthworm *Lumbricus Terrestris*. *J. Theor. Biol.* 210, 1871–1883.
- Quillin, K.J., 1999. Kinematic scaling of locomotion by hydrostatic animals: ontogeny of peristaltic crawling by the earthworm *Lumbricus Terrestris*. *J. Exp. Biol.* 202, 661–674.
- Ruppert, E.W., Barnes, R.D., 1994. *Invertebrate Zoology*, 6th Edition. Saunders College Publishing, Philadelphia.
- Skierczynski, B.A., Wilson, R.J.A., Kristan Jr., W.B., Skalak, R., 1996. A model of the hydrostatic skeleton of the leech. *J. Theor. Biol.* 329–342.
- Wadepuhl, M., 1989. Computer simulation of the hydrostatic skeleton. The physical equivalent, mathematics and application to worm-like forms. *J. Theor. Biol.* 136, 379–402.
- Walton, M., Jayne, B.C., Bennet, A.F., 1990. The energetic cost of limbless locomotion. *Science* 249, 524–527.